Robust State Estimation Based on Sliding Mode Observer for Aeroelastic System

In-Joo Jeong
Graduate Student, Department of Mechanical Engineering, Korea University,
Seoul 136-701, Korea

Sungsoo Na*
Associate Professor, Department of Mechanical Engineering, Korea University,
Seoul 136-701, Korea

Myung-Hyun Kim
Assistant Professor, Department of Naval Architecture and Ocean Engineering, Pusan University,
Pusan 609-735, Korea

Jae-Hong Shim
Associate Professor, Department of Mechatronics Engineering, Korea Polytechnic University,
Siheung City, Keonggi-do 429-793, Korea

Byung-Young Oh
Graduate Student, Department of Mechanical Engineering, Korea University,
Seoul 136-701, Korea

This paper concerns the application and demonstration of sliding mode observer for aeroelastic system, which is robust to model uncertainty including mass and stiffness of the system and various disturbances. The performance of a sliding mode observer is compared with that of a conventional Kalman filter to demonstrate robustness and disturbance decoupling characteristics. Aeroelastic instability may occur when an elastic structure is moving even in subcritical flow speed region. Simulation results using sliding mode observer are presented to control aeroelastic response of flapped wing system due to various external excitations as well as model uncertainty and sinusoidal disturbances in subcritical incompressible flow region.

Nomenclature

A   : System matrix for first order differential equation
α : Pitch angle
b   : Semi-chord
B   : Control input matrix

* Corresponding Author,
  E-mail : nass@korea.ac.kr
  TEL : +82-2-3290-3370; FAX : +82-2-926-9290
  Associate Professor, Department of Mechanical Engineering, Korea University, Seoul 136-701, Korea.
  (Manuscript **Received** June 3, 2004; **Revised** November 23, 2004)

β : Flap angle
c   : Nondimensional distance to flap hinge line from the elastic axis
d   : Nondimensional distance to elastic axis from leading edge
h ˙   : Plunging displacement
I_α, I_β : Inertia in pitch and of the flap
K   : Stiffness matrix
K_α, K_β, K_h : Stiffness of pitch, flap and plunge spring
M   : Mass matrix
S_α, S_β : Static moment of pitch and flap angle

$u(t)$: Control input vector

V or V_f : Flight speed

ρ : Density of fluid

w_G : Gust vertical velocity

Y : Column vector of plunge, pitch, and flap displacement

$[\ ]^T$: Transpose of a matrix

1. Introduction

The next generation of combat aircraft is likely to operate in more severe environmental conditions than in the past. This implies that such an aircraft, in addition to gust, will be exposed, among others, to blast, fuel explosion, and bomb firing. (Marzocca et al., 2001 : Librescu et al., 2004) Under such conditions, aeroelastic instability may happen when an elastic structure is moving even below flutter speed region. Moreover, in some special events, occurring during the operational life of the aircraft such as escape maneuvers, significant decays of the flutter speed can occur, with dramatic consequences for the further evolution of the aircraft. In this sense, robust feedback control methodology should be implemented for a stable operation, however, for aeroelastic system, due to unmeasurable aerodynamic lag states, proposing a vibration control scheme using full state feedback is not viable. In this connection, the use of a state estimator is a more practical way of developing active controller for aeroelastic system. All these facts fully underline the necessity of the implementation of an active control capability enabling one to fulfill two basic objectives : a) to enhance the subcritical aeroelastic response, in the sense of suppressing the wing oscillations in the shortest possible time, and b) to extend the flight envelop by suppressing the flutter instability and so, contributing to a significant increase of the allowable flight speed. With this in mind, in this paper the active aeroelastic control of a 3-DOF flapped wing system exposed to an incompressible flow field will be investigated. In this context, an LQG control strategy using sliding mode observer will be implemented, and some of its performances will be put into evidence that will be compared with conventional LQG with Kalman filter

2. Configuration of the Flapped Wing Model

Figure 1 presents the typical wing-flap that is considered in the present aeroelatic analysis (Scalan, 1951 ; Edwards, 1998). The three degrees of freedom associated with the airfoil appear clearly from Fig.1. The pitching and plunging displacements are restrained by a pair of springs attached to the elastic axis (EA) with spring constants K_α and K_h, respectively. The control flap is located at the trailing edge. A torsional flap spring of constant K_β is also attached at the hinge axis ; h denotes the plunge displacement (positive downward), α the pitch angle (measured from the horizontal at the elastic axis of the airfoil) and β is the flap deflection (measured from the axis created by the airfoil at the control flap hinge).
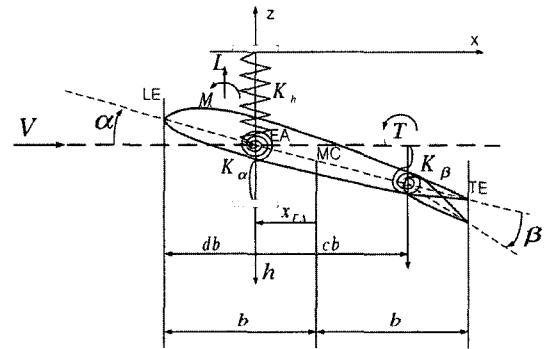

Fig. 1 Typical wing-flap section

3. Governing Equation of the Aeroelastic Model

In matrix form the aeroelastic governing equations of the 3-DOF flapped wing system can be written as : (Dowell, 1978 ; Edwards, 1998)

$$\mathbf{M}\ddot{y}(t) + \mathbf{K}y(t) = -\mathbf{L}(t) + \mathbf{L}_b\mathbf{f}(t) + \mathbf{L}_c u(t) \quad (1)$$

where $\mathbf{L}(t)$, $\mathbf{L}_b\mathbf{f}(t)$ and $\mathbf{L}_c u(t)$ represent the unsteady aerodynamic loads, blast and control loads, respectively.

In Eq. (1), the column vector of plunging/pitching/flapping displacement is defined as

$$\mathbf{y}(t) = [h(t) \ \alpha(t) \ \beta(t)]^T \qquad (2)$$

while

$$\mathbf{M} = \begin{bmatrix} m & S_\alpha & S_\beta \\ S_\alpha & I_\alpha & I_\beta + bcS_\beta \\ S_\beta & I_\beta + bcS_\beta & I_\beta \end{bmatrix} \qquad (3)$$

$$\mathbf{K} = \begin{bmatrix} K_h & 0 & 0 \\ 0 & K_\alpha & 0 \\ 0 & 0 & K_\beta \end{bmatrix} \qquad (4)$$

denote the mass, and stiffness matrices, respectively.

The corresponding second order aeroelastic governing equation can be cast in a first order state-space form as:

$$\dot{\mathbf{x}}(t) = \mathbf{A}\mathbf{x}(t) + \mathbf{B}u(t) + \mathbf{G}w(t) \qquad (5)$$

Here $\mathbf{A}$ is the aerodynamic matrix (Librescu et al., 2004), which is given in Appendix. The state vector is given by

$$\mathbf{x}(t) = [\dot{h}/b \ \dot{\alpha} \ \dot{\beta} \ h/b \ \alpha \ \beta \ B_1 \ B_2 \ A_1 \ A_2]^T \quad (6)$$

where $B_1 \ B_2 \ A_1 \ A_2$ denote aerodynamic lag states used to describe the state of the fluid which contain all the hereditary information about the aerodynamic system; $u(\text{t})$ is control input; $\mathbf{w}(t)$ is an external disturbance represented by a time-dependent external excitation, such as by a blast, sonic-boom or step pressure pulse; $\mathbf{G}$ is the disturbance-input matrix, while $\mathbf{B}$ is the control input matrix that is given by

$$\mathbf{B} = \frac{1}{I_\beta} [(\mathbf{M}^{-1}[0 \ 0 \ 1]^T)^T \ 0 \ 0 \ 0 \ 0 \ 0 \ 0]^T \qquad (7)$$

The new aerodynamic load vector appearing in Eq. (1) is expressed in terms of its components as

$$\begin{aligned} \mathbf{L}(t) &= [L_T(t) \ M_T(t) \ T_T(t)]^T \\ &= [L(t) + L_G(t) \ M(t) \\ &\quad + M_{yG}(t) \ T(t) + T_{yG}(t)]^T \end{aligned} \qquad (8)$$

where L, M, and T denote, respectively, the aerodynamic lift (measurement positive in the upward direction), the pitching moment about the one-quarter chord of the airfoil (positive nose-down) and the flap torque applied to the flap hinge.

The second terms in the expression (8) are due to the gust. In this respect, for the gust loading we have (Librescu et al., 2004)

$$L_G(t) = \frac{1}{2} \rho V^2 b \int_0^t I_{LG}(t-\sigma) \frac{w_G}{V} d\sigma \qquad (9)$$

$$M_{yG}(t) = \frac{1}{2} \rho V^2 b^2 \int_0^t I_{MG}(t-\sigma) \frac{w_G}{V} d\sigma \quad (10)$$

$$T_{yG}(t) = \frac{1}{2} \rho V^2 b^2 \int_0^t I_{fG}(t-\sigma) \frac{w_G}{V} d\sigma \quad (11)$$

where w_G is the gust vertical velocity, while I_{LG}, I_{MG}, and I_{fG} are the related impulse functions.

4. Linear Quadratic Gaussian Methodology

While the LQR design provides a robust controller, this control method is not practical due to the unmeasurable lag states for the present aeroelastic model. Furthermore, there are lots of chances when some sensors do not happen to work in a severe situation. Therefore, in general not all of the states are measured. In this connection, observer should be constructed in order to estimate the unmeasured states and the feedback control scheme should be implemented via the estimated states. In this sense, a set of estimator dynamic equation is designed as follows (Shim, 2004)

$$\dot{\hat{\mathbf{x}}}(t) = \mathbf{A}\hat{\mathbf{x}} + \mathbf{B}u(t) + \Lambda[\mathbf{y}(t) - \mathbf{C}\hat{\mathbf{x}}(t)] \quad (12)$$

$$u(t) = \Gamma\hat{\mathbf{x}}(t) \qquad (13)$$

where $\hat{\mathbf{x}}$ denotes the estimated state and Γ, Λ are the control gain matrix and the Kalman filter gain matrix, respectively. Furthermore, one needs to consider the effects of internal and external disturbances to the system. To address these issues, an LQG design, which uses noise-corrupted outputs for feedback, is used as a controller. Using LQG method with disturbance and sensor noise, the associated equations of motion corresponding to Eq. (5) is represented in state space form as:

$$\begin{aligned} \dot{\mathbf{x}}(t) &= \mathbf{A}\mathbf{x}(t) + \mathbf{B}u(t) = \mathbf{G}w(t) \\ \mathbf{y}(t) &= \mathbf{C}\mathbf{x}(t) + \pi(t) \end{aligned} \qquad (14)$$

The plant disturbance $\mathbf{w}(t)$ and sensor noise $\pi(t)$ are both assumed to be stationary, zero mean, Gaussian with joint correlation function

$$E\left\{\begin{bmatrix} \mathbf{w}(t) \\ \boldsymbol{\pi}(t) \end{bmatrix}[\mathbf{w}(t) \quad \boldsymbol{\pi}(t)]\right\} = \begin{bmatrix} \boldsymbol{\varXi} & 0 \\ 0 & \boldsymbol{\varTheta} \end{bmatrix}\delta(t-\tau) \quad (15)$$

where $E\{\cdot\}$ denotes the expected value, δ denotes the Kronecker delta, while $\boldsymbol{\varXi}$ and $\boldsymbol{\varTheta}$ denote the intensities of the disturbance and the sensor noise. For the present case, $\boldsymbol{\varXi}$ and $\boldsymbol{\varTheta}$ are defined as positive definite,

$$\boldsymbol{\varXi} = [\mathbf{I}_{10\times10}], \quad \boldsymbol{\varTheta} = [\mathbf{I}_{6\times6}] \quad (16)$$

The associated control input is obtained such that the system is stabilized and the control minimizes the cost function

$$J_{LQG} = E\left\{\int_0^\infty [\mathbf{x}^T \quad u^T]\begin{bmatrix} \mathbf{Z} & 0 \\ 0 & \mathbf{R} \end{bmatrix}\begin{bmatrix} \mathbf{x} \\ u \end{bmatrix}\right\}dt \quad (17)$$

where

$$Z = \begin{bmatrix} \mathbf{K} & 0 \\ 0 & \mathbf{M} \end{bmatrix}$$

The optimal feedback gain matrix $\varGamma$ and the Kalman filter gain matrix $\varLambda$ are obtained from

$$\varGamma = -\mathbf{R}^{-1}\mathbf{B}^T\mathbf{P}, \ \varLambda = -\prod\mathbf{C}^T\boldsymbol{\varTheta}^{-1} \quad (18)$$

where $\mathbf{P}$ and $\prod$ are the positive definite solutions of the following Riccati equations :

$$\mathbf{A}^T\mathbf{P} + \mathbf{P}\mathbf{A} - \mathbf{P}\mathbf{B}\mathbf{R}^{-1}\mathbf{B}^T\mathbf{P} + \mathbf{Z} = 0 \quad (19)$$

$$\mathbf{A}\prod + \prod\mathbf{A}^T - \prod\mathbf{C}^T\boldsymbol{\varTheta}^{-1}\mathbf{C}\prod + \mathbf{G}\boldsymbol{\varXi}\mathbf{G}^{-1} = 0 \quad (20)$$

5. Robust State Observer

Since unmeasured states are not considered in the controller and observer design, their neglect may cause both control spillover and observation spillover. Spillover effects are undesirable and may cause system instability (Balas, 1978) and reduction in performance (Inman, 2000). Although the effects of control and observation spillover do not always produce instability, it is desirable to reduce the observation spillover as to remove the potential to generate any instability. To this end, we introduce both Kalman filter (KF) and sliding mode observer. It is common to estimate the states using a Kalman filter in stochastic case. This observer provides state estimates from the input, the output, and the mathematical model of the system under consideration. It should be noted that the mathematical model

is assumed to be exact and disturbances on the physical system have been ignored. In this connection, an estimator sometimes may be dangerous, and it is desirable for the estimator to possess robustness. In this sense, *sliding mode observer* (SMO) is introduced and reduces the effect of observation spillover from the unmeasured states, which is known to have the robustness property and disturbance decoupling property. In this sense, a sliding mode observer is designed to provide estimates of state (Edwards, 1998). The sliding mode observer has the form (Na, 2004)

$$\dot{\hat{\mathbf{x}}} = \mathbf{A}\hat{\mathbf{x}} + \mathbf{B}u(t) + \varLambda(y(t) - \mathbf{C}\hat{\mathbf{x}}) + \gamma v(t) \quad (21)$$

where $v(t)$ represents a discontinuous switching component defined as (Edwards, 1998)

$$v(t) = \begin{cases} -\rho\dfrac{\mathbf{T}e}{\|\mathbf{T}e\|} & e\neq0 \\ 0 & e=0 \end{cases} \quad (22)$$

The matrix $\mathbf{T}$ is a positive definite symmetric matrix, and $\mathbf{A}_0 = \mathbf{A} - \varLambda\mathbf{C}$ satisfies

$$\mathbf{T}\mathbf{A}_0 + \mathbf{A}_0^T\mathbf{T} = -\mathbf{Q} \quad (23)$$

for some positive definite design matrix $\mathbf{Q}$, and ρ is a positive scalar function.

The objective is to induce a sliding motion in the error space

$$S_0 = \{e \in \mathbb{R}^n : \mathbf{C}e = 0\} \quad (24)$$

that consequently drives the error $e = \hat{\mathbf{x}} - \mathbf{x}$ to zero in finite time despite the presence of the uncertainties in modeling and disturbances. The error dynamics become

$$\dot{e} = \mathbf{A}_0 e + \gamma v - \mathbf{G}\mathbf{w} \quad (25)$$

Note that external excitation appear as disturbances in the error dynamics. With the given form of additional discontinuous input v, the sliding mode observer can estimate the states of the system. For the stability of observation error dynamics considering external excitations, using the Lyapunov stability theory, it can be shown that the error dynamics Eq. (25) are asymptotically stable.

6. Discussion of Results

The considered geometrical and physical char-

Table 1 Geometrical Parameters of Wing Model

| parameter = value	parameter = value
$b = 0.3048$ (m)	$c = 1.0$
$x_{EA} = -0.3$	$m = 128.7$ (kg/m)
$K_a = 0.2 \times 100^2 I_a$	$I_a = 0.25 \times 26.9$ (kg-m²/m)
$K_\beta = 0.2 \times 300^2 I_\beta$	$I_\beta = 0.25 \times 0.6727$ (kg-m²/m)
$K_h = 0.2 \times 50^2$ m	$S_a = 0.3 \times 8.946$ (kg)
$\rho = 1.225$ (kg/m³)	$S_\beta = 0.3 \times 1.471$ (kg)

acteristics of the 3-DOF wing-flap system are identical to the ones in the work by Shim (2004).

The geometrical and physical characteristics of the 3-DOF flapped wing system to be used in the present numerical simulations are presented in Table 1. The flutter speed for this model is $V_F = 139.3$ m/sec. In order to validate the result present in this paper a comparison is done using the parameters shown in Olds (1997) and York (1980), for which the calculated flutter speed is $V_F = 271.3$ m/sec. The critical value of the flutter speed is obtained herein via the solution of both the complex eigenvalue problem and from the subcritical aeroelastic response analysis and an excellent agreement with Olds (1997) and York (1980) is reached. As remarked in Djayapertapa (2002), from mathematical point of view, it can be assumed that, instead of moving the flap with a required deflection, an equivalent control hinge moment can be incorporated into the open-loop aeroelastic governing equation (5). This is analytically valid since this external moment acts on the flap-hinge and affects only β DOF. The following numerical simulations are based on initial conditions $\tilde{h} = 0.01$ and $a = 0.1$ rad with flight speed $V_f = 131$ m/sec.

6.1 The performance of observer in terms of number of states available

In general, all of the states are not available online due to either initial configuration or malfunctions.

We can consider the case which it is possible to measure only both velocity and displacement of h and a as a function of time. The associated output equation is given by
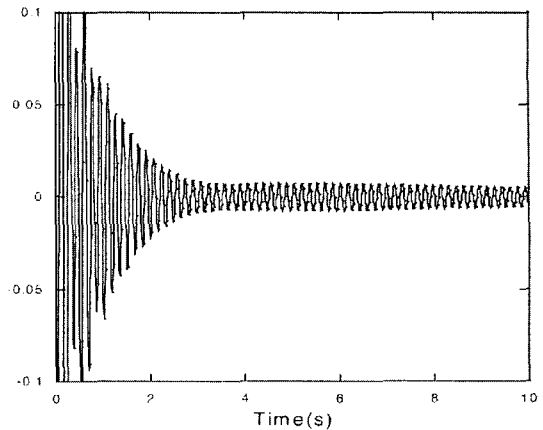
Fig. 2 Performance of estimation of plunging state based on pitching measurement via KF

$$\mathbf{y}(t) = \mathbf{C}\mathbf{x}(t), \ \mathbf{C} = \begin{bmatrix} 1 & 0 & 0 & 0 & 0 & 0 & 0 & 0 & 0 \\ 0 & 1 & 0 & 0 & 0 & 0 & 0 & 0 & 0 \\ 0 & 0 & 0 & 1 & 0 & 0 & 0 & 0 & 0 \\ 0 & 0 & 0 & 0 & 1 & 0 & 0 & 0 & 0 \end{bmatrix} \quad (26)$$

We may also invoke more terrible situations where it is possible to measure only plunging displacement h, which can be represented by output equation

$$\mathbf{y}(t) = \mathbf{C}\mathbf{x}(t), \ \mathbf{C} = [0 \ 0 \ 0 \ 1 \ 0 \ 0 \ 0 \ 0 \ 0] \quad (27)$$

The other one is the case to measure only pitching displacement a, which can be given by

$$\mathbf{y}(t) = \mathbf{C}\mathbf{x}(t), \ \mathbf{C} = [0 \ 0 \ 0 \ 0 \ 1 \ 0 \ 0 \ 0 \ 0] \quad (28)$$

The following figures are represented by error $e = \hat{\mathbf{x}} - \mathbf{x}$, which is the difference between actual state and estimated state.

Figure 2 displays the performance of estimation of plunging state using Kalman filter, which is based on pitching measurement. The result shows after far more than 10 seconds the Kalman filter can accurately recover the nondimensional state $\tilde{h}(= h/b)$. Figure 3 represents the Kalman filter's performance of estimation of pitching state using measurement of plunging displacement. Finally, the stable estimation is reached, which takes more than twice of the case of Fig. 2. Figure 4 is pitching state error based on four state measurements such as $\dot{\tilde{h}}$, $\dot{a}$, $\tilde{h}$, a. As expected, performance of recovering estimation of state is
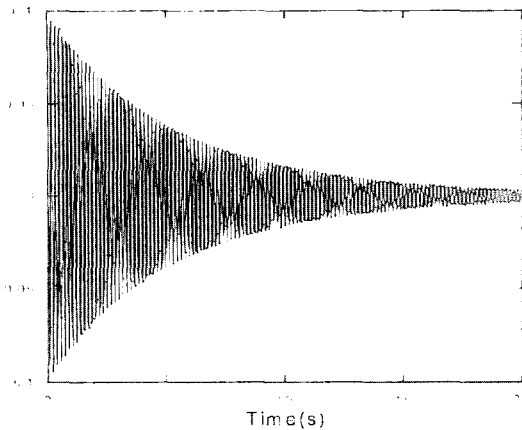
Fig. 3 Performance of estimation of pitching state based on plunging measurement via KF
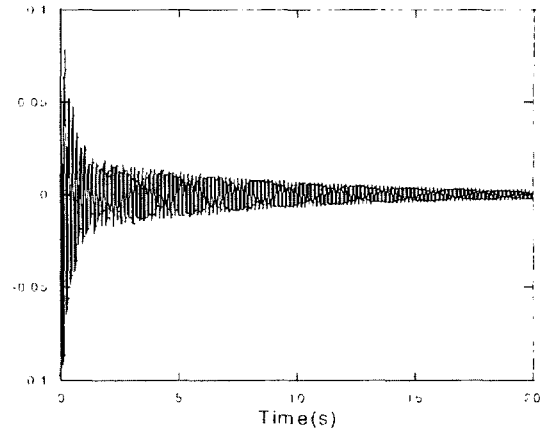

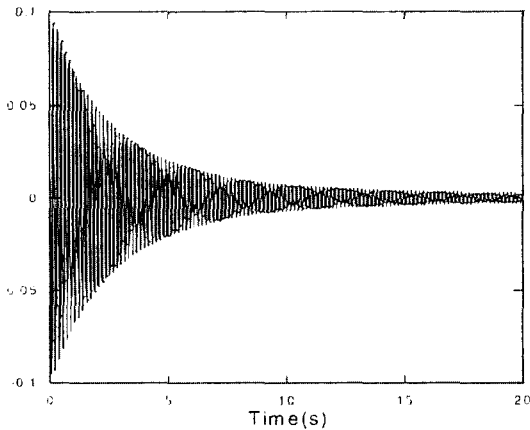**Fig. 5** Performance of estimation of pitching state based on plunging measurement via SMO

Fig. 4 Performance of estimation of pitching state based on both plunging and pitching measurements via KF

excellent compared to the one based on only one measurement of plunging displacement, which is the case of Fig. 3.

6.2 Performance of observers using one measurement

As mentioned before, many harsh situations may occur when only one state is available due to sensor failure. However, the observer should estimate the other states with one measurement so that the system is to survive, and the feedback control scheme should be implemented via the estimated states. In this connection, the sliding mode observer is introduced and performances

will be put into evidence that will be compared with conventional Kalman filter.

Figure 5 represents the performance of estimation of pitching state using sliding mode observer, which is based on plunging measurement. The result shows that sliding mode observer successfully recover the nondimensional state $\bar{h}$ $(=h/b)$ in several seconds. The performance of sliding mode observer is excellent compared to the one of Kalman filter (Fig. 3) in severe conditions using only one measurement. The other case of estimation of plunging state based on pitching measurement is not shown here. The performance of stable estimation of plunging state is similar as the one before.

6.3 Performance of observers subjected to model uncertainty

The robustness of the observers and the performance of the state estimation were tested by changing mass of the mathematical model on which the observers are based, which may simulate the robustness of observers subjected to model uncertainty
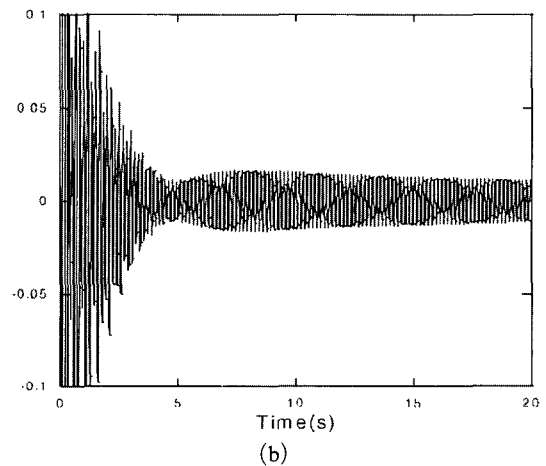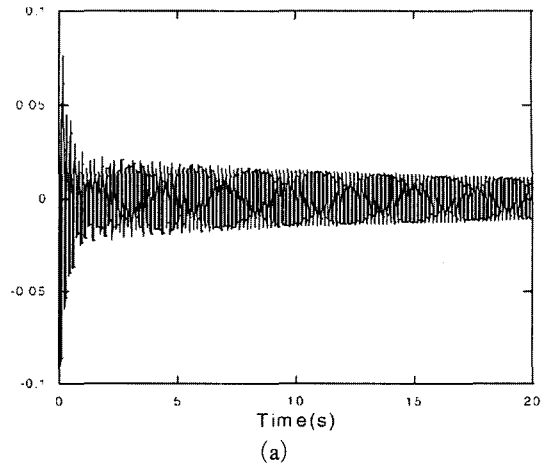
Figure 6(a) and (b) show the state estimation as a function of time with Kalman filter designed based on an incorrect mathematical model. Figure 6(a) displays the pitching state error based on plunging measurement, while Fig. 6(b) depicts the plunging state error based on pitching measurement. With the incorrect model, the Kalman
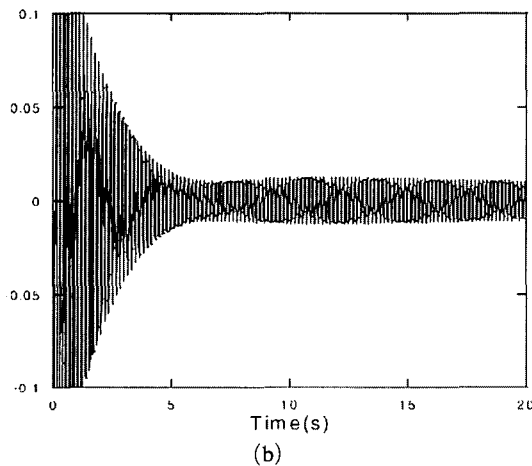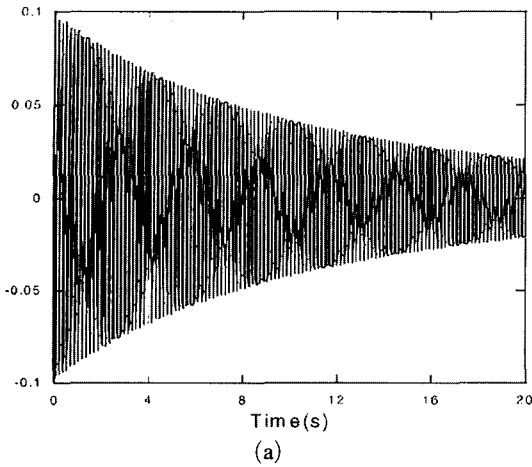
Fig. 6 Performance of estimation of state based on only one measurement via KF with 10% mass reduction

Fig. 7 Performance of estimation of state based on only one measurement via SMO with 10% mass reduction

filter produced a stable estimation in far more than 20 sec (the case of (a)), and 10 sec (the case of (b)), respectively. Compared with the results Fig.2 and Fig. 3 obtained by correct model, it would take a longer time for a stable estimation with incorrect model than the one with correct one. In a certain sense, Kalman filter fails as observer in mission with restricted sensor measurement.

Figure 7(a) and (b) depict the state estimation error as a function of time with sliding mode observer designed based on an incorrect mathematical model. Figue 7(a) displays the pitching state estimation based on plunging measurement, while Fig. 7(b) shows the plunging state estima-

tion based on pitching measurement. Even with the incorrect model, the sliding mode observer produced a stable estimation, which implies robustness of observer subjected to model uncertainty and also proves excellence of state estimation compared to conventional Kalman filter.

7. Conclusions

The present research investigates the performance of a sliding mode observer for state estimation in an aeroelastic system. Performance comparisons are made with the conventional Kalman filter. We also examined the performance of observer based on only one sensor measurement.

The sliding mode observer recovers the state more rapidly than the Kalman filter does. In addition, robust performance of stable state estimation in the presence of uncertainties is achieved using sliding mode observer. Since performance of feedback control system definitely depends on the estimation quality, satisfactory state estimation and robust performance of the sliding mode observer were demonstrated for aeroelastic system.

Acknowledgment

References

Balas, M. J., 1978, "Feedback Control of Flexible Systems," *IEEE Transactions on Automatic Control* AC-23(4), pp. 673~679.

Chung, Chan-Hoon, 2003, "Aeroelastic Response of 2-D Wing System Using Active Control," MS Thesis, Department of Mechanical Engineering, Korea University, Korea.(in Korea)

Djayapertapa, L. and Allen, C. B., 2002, "Numerical Simulation of Active Control of Transonic Flutter," *Proc. Of the 23rde ICAS Congress*, Toronto, 411.1-411.10

Dowell, E. H., 1978, *A Modern Course in Aeoelasticity*, Sijthoff and Noordhoff,.

Edwards, C. and Spurgeon, S., 1998, Sliding Mode Control : Theory and Applications, The Taylor & Francis.

Inman, D. J., 2000, "Active Modal Control for Smart Structures," *Philosophical Transanctions : Mathematical, Physical & Engineering Sciences* 359(1778), pp. 205~219.

Kim, M. H. and Inman, D. J., 2001, "Reduction of Observation Spillover in Vibration Suppression Using a Sliding Mode Observer," *J. of Vibration and Control*, 7, pp. 1087~1105.

Librescu, L., Na, S., Marzocca, P., Chung, C. and Kwak, M., 2004, "Active Aeroelastic Control of 2-D Wing-Flap Systems Operating in an Incompressible Flowfield and Impacted by a Blast Pulse," *Journal of Sound and Vibration.*(in press)

Marzocca, P., Librescu, L. and Chiocchia, G., 2001, "Aeroelastic Response of a 2-D Lifting Surfaces to Gust and Arbitrary Explosive Loading Signatures," *International Journal of Impact Engineering*, Vol. 25, No. 1, pp. 41~65.

Na, S., Librescu, L., Marzocca, P., Kim, M. H. and Jeong, I., 2004, "Aeroelastic Response of Flapped Wing Systems Using Robust Conrol Methodology," 45th AIAA/ASME/ASCE/AHS/ASC Structures, Structural Dynamics, and Materials Conference, CD-Rom version.

Olds, S. D., 1997, "Modeling and LQR Control of a Two-Dimensional Airfoil," MS Thesis, Department of Mathematics, Virginia Polytechnic Institute and State University, Blacksburg, VA.

Scanlan, R. H. and Rosenbam, R., 1951, *Introduction to the Study of Aircraft Vibration and Flutter*, The Macmillan Co.

Shim, J., Na, S. and Chung, C., 2004, "Aeroelastic Response of an Airfoil-Flap System Exposed to Time-Dependent Disturbances," *KSME International Journal*, Vol. 18, No. 4, pp. 560~572.

York, D. L., 1980, "Analysis of Flutter and Flutter Suppression via an Energy Method," MS Thesis, Department of Aerospace and Ocean Engineering, Virginia Polytechnic Institute and State University, Blacksburg, VA., U.S.A.

Appendix

Aerodynamic matrix $\mathbf{A}$ is given as follows :

$$\mathbf{A} = \begin{bmatrix} \mathbf{A}_{11} & \mathbf{A}_{12} & \mathbf{A}_{13} \\ \mathbf{A}_{21} & \mathbf{A}_{22} & \mathbf{A}_{23} \\ \mathbf{A}_{31} & \mathbf{A}_{32} & \mathbf{A}_{33} \end{bmatrix}$$

where

$$\mathbf{A}_{11} = -[\mathbf{M} + \pi\rho b^2 \mathbf{Z}_1]^{-1} \pi\rho b^2 \mathbf{Z}_2$$

$$\mathbf{A}_{12} = -[\mathbf{M} + \pi\rho b^2 \mathbf{Z}_1]^{-1} (\mathbf{K} + \pi\rho b^2 \mathbf{Z}_3)$$

$$\mathbf{A}_{13} = -[\mathbf{M} + \pi\rho b^2 \mathbf{Z}_1]^{-1} \pi\rho b^2 \mathbf{Z}_4$$

$$\mathbf{A}_{21} = \mathbf{I}_{3\times3}, \ \mathbf{A}_{22} = \mathbf{0}_{3\times3}, \ \mathbf{A}_{23} = \mathbf{0}_{3\times4}$$

$$\mathbf{A}_{31} = \begin{bmatrix} [R_1 \; R_2 \; R_3]\mathbf{A}_{11} + [0 \; R_4 \; R_5] \\ [R_1 \; R_2 \; R_3]\mathbf{A}_{11} + [0 \; R_4 \; R_5] \\ [R_6 \; R_7 \; R_8]\mathbf{A}_{11} + [0 \; R_9 \; R_{10}] \\ [R_6 \; R_7 \; R_8]\mathbf{A}_{11} + [0 \; R_9 \; R_{10}] \end{bmatrix}$$

$$\mathbf{A}_{33} = \begin{bmatrix} \begin{bmatrix} \dfrac{-\beta_1 V}{b} & 0 & 0 & 0 \\ 0 & \dfrac{-\beta_1 V}{b} & 0 & 0 \\ 0 & 0 & \dfrac{-\beta_1 V}{b} & 0 \\ 0 & 0 & 0 & \dfrac{-\beta_1 V}{b} \end{bmatrix} + \begin{bmatrix} [R_1 \; R_2 \; R_3]\mathbf{A}_{13} \\ [R_1 \; R_2 \; R_3]\mathbf{A}_{13} \\ [R_6 \; R_7 \; R_8]\mathbf{A}_{13} \\ [R_6 \; R_7 \; R_8]\mathbf{A}_{13} \end{bmatrix} \end{bmatrix}$$

$$\mathbf{Z}_1 = \begin{bmatrix} b & -ba & \dfrac{b}{2\pi}\Phi_4 \\ -ab^2 & b^2\left(\dfrac{1}{8}+a^2\right) & \dfrac{b^2}{4\pi}\Phi_7 \\ \dfrac{b^2}{2\pi}\Phi_4 & \dfrac{b^2}{4\pi}\Phi_7 & \dfrac{b^2}{4\pi^2}\Phi_{12} \end{bmatrix}$$

$$\mathbf{Z}_2 = \begin{bmatrix} 2V & 2V(1-a) & \dfrac{V}{\pi}(\Phi_3+\Phi_2) \\ -V(2a+1) & -aVb(1-2a) & \dfrac{Vb}{2\pi}[\Phi_4-(2a+1)\Phi_2] \\ \dfrac{Vb}{\pi}\Phi_4 & \dfrac{Vb}{\pi}\left[\dfrac{\Phi_9}{2}+\Phi_8\left(\dfrac{1}{2}-a\right)\right] & \dfrac{Vb}{2\pi^2}(\Phi_{21}+\Phi_2\Phi_8) \end{bmatrix}$$

$$\mathbf{Z}_3 = \begin{bmatrix} 0 & \dfrac{2V^2}{b} & \dfrac{2V^2}{\pi b}\Phi_1 \\ 0 & -V^2(2a+1) & \dfrac{V^2}{\pi}[\Phi_5-(2a+1)\Phi_1] \\ 0 & \dfrac{V^2}{\pi}\Phi_8 & \dfrac{V^2}{\pi^2}(\Phi_{10}+\Phi_1\Phi_8) \end{bmatrix}$$

$$\mathbf{Z}_4 = \begin{bmatrix} -\dfrac{2V\alpha_1}{b} & -\dfrac{2V\alpha_2}{b} & 0 & 0 \\ 0 & 0 & 0 & 0 \\ 0 & 0 & -\dfrac{V\alpha_1}{b} & -\dfrac{V\alpha_2}{b} \end{bmatrix}$$

Herein, R_i and Φ_i are listed in Chung (2003).